International Journal of Heat and Mass Transfer 53 (2010) 1691–1698

Contents lists available at ScienceDirect

International Journal of Heat and Mass Transfer

journal homepage: www.elsevier.com/locate/ijhmt

Visualization of heat flow using Bejan's heatline due to natural convection of water near 4 °C in thick walled porous cavity

Yasin Varol [a], Hakan F. Oztop [a], Moghtada Mobedi [b], Ioan Pop [c,*]

[a] Department of Mechanical Education, Firat University, 23119 Elazig, Turkey
[b] Department of Mechanical Engineering, Izmir Institute of Technology, 35430 Izmir, Turkey
[c] Faculty of Mathematics, University of Cluj, CP 253, 3400 Cluj, Romania

ARTICLE INFO

Article history:
Received 8 July 2009
Received in revised form 6 November 2009
Accepted 10 November 2009

Keywords:
Heatline
Maximum density
Conjugate
Natural convection

ABSTRACT

A numerical study on natural convection heat transfer of cold water near 4 °C in a thick bottom walled cavity filled with a porous medium has been performed. It is assumed that the cavity is isothermally heated from the outside of the thick bottom wall and cooled from ceiling. The finite-difference method has been used to solve the governing partial differential equations of heat and fluid flow. Effects of thermal conductivity ratio, Rayleigh number and bottom wall thickness on heat transfer from the bottom to the ceiling have been studied. The heatline visualization technique has been used to demonstrate the path of heat transport through the enclosure. Moreover, streamlines and isotherms have been used to present fluid flow and temperature distributions. The obtained results show that multiple circulation cells are formed in the cavity and the local Nusselt numbers at the bottom wall and solid–fluid interface are highly affected by formed cells. The increase of Rayleigh number and thermal conductivity ratio increases heat transfer through the cavity. However, the increase of thickness of the bottom wall reduces the mean Nusselt number. Almost one-dimensional conduction heat transfer is observed in the solid bottom wall of the cavity.

1. Introduction

Analysis of thermal energy transport through porous media has many important applications in engineering, such as the energy efficient building design, geothermal reservoirs, nuclear industry, etc. Most of these applications can be found in the published books [1,2]. An interesting result in these applications is that there is a non-linear relationship between the density of water and the temperature around 3.98 °C. At this point the density of water has a maximum value and the Boussinesq approximation is not valid [3]. In this respect, Blake et al. [4] performed a numerical study on natural convection in a two-dimensional horizontal porous layer heated from below and saturated with cold water at the maximum density of water at 3.98 °C inside the layer, while the temperature of the top surface is maintained at 0 °C and the temperature of the bottom surface is changed from 4 °C to 8 °C, respectively. It is found that the number of cells is affected when the values of the Rayleigh number are changed. Saeid and Pop [5] performed a numerical analysis to investigate the effects of maximum density on natural convection in a partially heated cavity. It is worth mentioning that relatively many studies can be found in the literature on natural convection in cavities filled with a Newtonian fluid or a porous medium saturated with water near 4 °C, see Sivasankaran and Ho [6], Osorio et al. [7], Inaba and Fukuda [8], Lin and Nansteel [9], Ho and Tu [10].

In many thermal systems, both conduction in the solid (such as a wall, fin, etc.) and convection in the fluid region occur simultaneously and these are called as conjugate heat transfer problems. The influence of heat conduction in a wall, on natural convection in a cavity filled with a porous medium has gained the attention of several researchers in recent years. Saeid [11] performed a numerical study to investigate the effect of heat conduction of a vertical wall on free convection in a porous cavity. It has been found that either increasing the Rayleigh number and the thermal conductivity ratios or decreasing the thickness of the bounded wall can increase the average Nusselt number. The natural convection in a square cavity with the two horizontal walls of finite thickness and filled with a porous medium has been investigated numerically by Baytas et al. [12]. It has been shown that the value of the mean Nusselt number decreases with the increase of thermal conductivity ratio. Al-Amiri et al. [13] considered the steady-state conjugate natural convection in a fluid-saturated porous cavity. The configuration consists of two insulated horizontal walls and two vertical walls one of which has a finite thickness. The vertical walls are maintained at constant but different temperatures. Finally, we mention the paper by Chang and Lin [14], who studied

* Corresponding author. Tel.: +40 264 594315; fax: +40 264 591906.
E-mail addresses: pop.ioan@yahoo.co.uk, pop.ioan30@yahoo.com, pop.ioan@hotmail.com (I. Pop).

0017-9310/$ - see front matter © 2010 Elsevier Ltd. All rights reserved.
doi:10.1016/j.ijheatmasstransfer.2010.01.020

Nomenclature

AR	aspect ratio parameter, $AR = H/L$
g	magnitude of the gravitational acceleration (m s^{-2})
H	height of the cavity (m)
h'	thickness of the bottom wall (m)
h	heat transfer coefficient, dimensionless thickness of the bottom wall, $h = h'/H$
k	thermal conductivity (W/m °C)
K	permeability of the porous medium (m^2)
L	length of the cavity (m)
Nu_x	local Nusselt number, $Nu_x = (-\partial\theta/\partial Y)_{Y=0}$
Nu	mean Nusselt number as in Eqs. (21) and (22)
Ra	Rayleigh number, $Ra = (g\beta K(T_h - T_c)L)/\upsilon\alpha_m$
T	temperature, °C
u, v	dimensional velocities in x- and y-directions (m s^{-1})
U, V	dimensionless velocities in X- and Y-directions
x, y	dimensional coordinates (m)
X, Y	dimensionless coordinates

Greek letters

α_m	effective thermal diffusivity (m^2 s^{-1})
β	thermal expansion coefficient (K^{-1})
γ	constant in Eq. (4)
κ	conjugate parameter, $\kappa = k_s/k_f$
ϕ	dimensionless heat function
Φ	any variable
θ	dimensionless temperature, $\theta = (T - T_m)/(T_h - T_c)$
ρ	density (kg m^{-3})
υ	kinematic viscosity (m^2 s^{-1})
Ψ	dimensionless stream function, $\Psi = \psi/\alpha_m$

Subscripts

c	cold
f	fluid
h	hot
s	solid
m	maximum

the effect of the conduction of a wall on natural convection in a cavity filled with a non-Darcian porous medium.

The heatline visualization technique is a useful tool for conjugate heat transfer problems to show the path of heat transfer from solid to fluid or vice verse. The technique was first proposed by Kimura and Bejan [15] to visualize heat transport for a convective heat transfer. A detailed review on the application of heatline visualization method has been presented by Costa [16]. Hakyemez et al. [17] used heatline visualization technique to show the path of heat transfer in a cavity. In their geometry, the ceiling wall behaves as a thermal barrier.

Based on the existing literature, it seems that no study has been performed on the conduction-natural convection heat transfer in a cavity filled with a porous medium and saturated with cold water. The aim of the present study is, therefore, to examine the conduction and natural convection heat transfer in a cavity with a thick bottom wall for the case when the cavity is heating by the bottom wall and is cooled by the ceiling. The obtained results are discussed for some values of the thicknesses parameter of the bottom wall, Rayleigh numbers and thermal conductivity ratios parameter.

2. Governing equations and model

A two-dimensional horizontal rectangular cavity of height H and length L with the vertical walls adiabatic and a thick bottom wall of thickness h' is considered as shown in Fig. 1. It is assumed that the cavity is filled with a porous layer saturated with water at a maximum. In addition, it is assumed that the cavity is heated from the bottom wall and cooled from the ceiling. The governing equations of continuity, Darcy and energy can be written as follows:

$$\frac{\partial u}{\partial x} + \frac{\partial v}{\partial y} = 0, \tag{1}$$

$$\frac{\partial u}{\partial y} - \frac{\partial v}{\partial x} = -\frac{2gK\gamma(T - T_m)}{\upsilon}\frac{\partial T}{\partial x}, \tag{2}$$

$$u\frac{\partial T}{\partial x} + v\frac{\partial T}{\partial y} = \alpha_m\left(\frac{\partial^2 T}{\partial x^2} + \frac{\partial^2 T}{\partial y^2}\right), \tag{3}$$

where u and v are the velocity components along the x- and y-axes, K is the permeability of the porous medium, α_m is the effective thermal diffusivity of the porous medium and υ represents the kinematic viscosity. The following assumptions are used to write Eqs. (1)–(3):

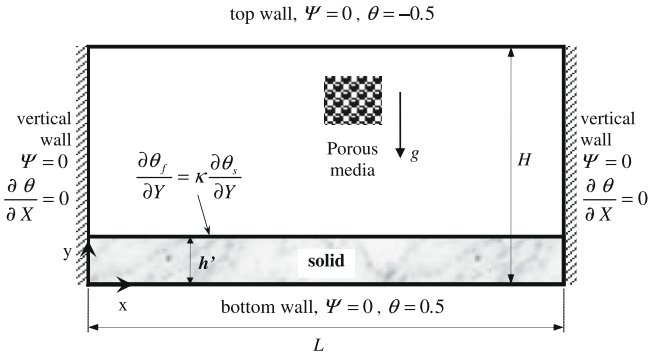

Fig. 1. Physical model.

- the viscous drag and inertia terms are neglected;
- the flow is two-dimensional and steady;
- the fluid is incompressible;
- radiation mode of heat transfer is neglected compared to other modes of heat transfer;
- the dependence of density ρ on temperature of the porous medium saturated with cold water is given by Goren [18] as

$$\frac{\rho - \rho_m}{\rho_m} = -\gamma(T - T_m)^2, \tag{4}$$

where ρ_m and T_m are the maximum density and the maximum temperature in the liquid phase, respectively. The symbol γ is the constant coefficient and its value is taken as $\gamma = 8.0 \times 10^{-6}$ °C^{-2}. Moore and Weiss [19] stated that Eq. (4) is accurate to within ±4% in the range $0\ °C \leqslant T \leqslant 8\ °C$ and the value of maximum temperature is taken as $T_m \cong 4$ °C. Further, the following dimensionless variables can be introduced to obtain the dimensionless form of the governing equations (Eqs. (1)–(3)):

$$X = \frac{x}{L}, \quad Y = \frac{Y}{L}, \quad U = \frac{uL}{\alpha_m}, \quad V = \frac{vL}{\alpha_m}, \quad \theta = \frac{T - T_m}{T_h - T_c}, \tag{5}$$

and the dimensionless stream function Ψ, which is defined in the usual way as

$$U = \frac{\partial \Psi}{\partial Y}, \quad V = -\frac{\partial \Psi}{\partial X} \tag{6}$$

Substituting (5) into Eqs. (1)–(3) and using Eq. (6), leads to the following set of equations [20–21]:

$$\frac{\partial^2 \Psi}{\partial X^2} + \frac{\partial^2 \Psi}{\partial Y^2} = -2Ra\frac{\partial \theta}{\partial X}\theta, \tag{7}$$

$$\frac{\partial \Psi}{\partial Y}\frac{\partial \theta}{\partial X} - \frac{\partial \Psi}{\partial X}\frac{\partial \theta}{\partial Y} = \frac{\partial^2 \theta}{\partial X^2} + \frac{\partial^2 \theta}{\partial Y^2}, \tag{8}$$

where Ra is the Rayleigh number for a porous medium which is defined as:

$$Ra = \frac{gK\gamma(T_h - T_c)^2 L}{\nu \alpha_m}. \tag{9}$$

In addition, the following heat conduction equation is valid for the heat transfer in the solid wall:

$$\frac{\partial^2 \theta_s}{\partial X^2} + \frac{\partial^2 \theta_s}{\partial Y^2} = 0, \tag{10}$$

where θ_s denotes the dimensionless temperature in the solid wall.

2.1. Definition of heat function

Heat function for a two-dimensional convection problem can be defined as [22]

$$-\frac{\partial h}{\partial x} = \rho c_p v(T - T_m) - k_f \frac{\partial T}{\partial y}, \tag{11}$$

$$\frac{\partial h}{\partial y} = \rho c_p u(T - T_m) - k_f \frac{\partial T}{\partial x}, \tag{12}$$

where h is the dimensional heat function, k_f is the thermal conductivity of the fluid-saturated porous medium and c_p is the specific heat at constant pressure. By employing the dimensionless parameters defined by Eq. (5), the dimensionless form of Eqs. (11) and (12) become:

$$-\frac{\partial \phi}{\partial X} = V\theta - \frac{\partial \theta}{\partial Y}, \tag{13}$$

$$\frac{\partial \phi}{\partial Y} = U\theta - \frac{\partial \theta}{\partial X}, \tag{14}$$

where ϕ is the dimensionless heat function and it is defined as:

$$\phi = \frac{h}{k(T_h - T_c)}. \tag{15}$$

Assuming that h is a continuous function to its second order derivatives, Eqs. (13) and (14) lead to the following differential equation for the heat function:

$$\frac{\partial^2 \phi}{\partial X^2} + \frac{\partial^2 \phi}{\partial Y^2} = \frac{\partial (U\theta)}{\partial Y} - \frac{\partial (V\theta)}{\partial X}. \tag{16}$$

The convection terms which are written on the right-hand side of Eq. (16) act as a source term. For the solid region, the value of source term is zero due to fact that the velocity is absent here. We notice that the solution of the heat function equation (16) yields the distribution of the dimensionless heat function in the cavity. The drawing of isolines of the heat function generates the heatlines.

2.2. Boundary conditions

For all solid walls, the boundary conditions for the stream function Ψ are given as $\Psi = 0$, however, the boundary conditions for the energy equation are not identical at all walls. As indicated by Saeid and Pop [5] that definition of dimensional boundary conditions are taken as $T_c = 0\,^\circ C$ and $T_h = 8\,^\circ C$ for cold and hot walls, respectively. Thus, non-dimensional boundary conditions as

$$\text{On the bottom wall (hot)}: \quad \theta = 0.5, \tag{17}$$

$$\text{On the side walls (adiabatic)}: \quad \frac{\partial \theta}{\partial n} = 0, \tag{18}$$

$$\text{On the top wall (cold)}: \quad \theta = -0.5. \tag{19}$$

The boundary condition for the solid–fluid interface of the bottom wall is defined as:

$$\frac{\partial \theta_f}{\partial Y} = \kappa \frac{\partial \theta_s}{\partial Y}, \tag{20}$$

where $\kappa = k_s/k_f$ is the conjugate parameter. The physical quantities of interest are the local Nusselt number Nu_x and the average Nusselt number, Nu. For the fluid region the local and average Nusselt numbers are defined as:

$$Nu_{xf} = -\left(\frac{\partial \theta}{\partial Y}\right)_{Y=h}, \quad Nu_f = \int_0^1 Nu_{xf}\, dX. \tag{21}$$

While for the solid region local and average Nusselt numbers can be defined as:

$$Nu_{xs} = -\left(\frac{\partial \theta_s}{\partial Y}\right)_{Y=0}, \quad Nu_s = \int_0^1 Nu_{xs}\, dX. \tag{22}$$

For the present problem, the vertical sides of the wall are insulated; therefore the relation between mean Nusselt numbers for solid and fluid regions can be expressed as:

$$Nu_f = \kappa Nu_s. \tag{23}$$

The boundary conditions for the dimensionless heatfunction equation (Eq. (16)) are obtained from the integration of differential definition of Φ along the considered boundary conditions:

$$\text{for } X = 0 \text{ adiabatic wall}: \quad \phi(0, Y) = \phi(0, 0), \tag{24}$$

$$\text{for } X = 1 \text{ adiabatic wall}: \quad \phi(1, Y) = \phi(1, 0), \tag{25}$$

$$\text{for } Y = 0 \text{ hot wall}: \quad \phi(X, 0) = \phi(0, 0) + \kappa \int_0^X Nu_{xs}\, dX, \tag{26}$$

$$\text{for } Y = H/L \text{ cold wall}: \quad \phi(X, H/L) = \phi(0, H/L) + \int_0^X Nu_{xf}\, dX. \tag{27}$$

For the solid–fluid interface the boundary condition for the heat function ϕ can be obtained from the following relation:

$$\text{for } Y = h \quad \text{and} \quad 0 < X \leqslant 1 \frac{\partial \phi}{\partial X} = \frac{\partial \theta}{\partial Y}. \tag{28}$$

The value of heat function at the origin point is assumed as $\phi(0, 0) = 0$.

3. Numerical method

Finite difference method with central difference technique is used to solve the governing equations (7) and (8) subject to the boundary conditions (17)–(20). For boundaries, backward and forward difference schemes were applied. The solution of linear algebraic equations was performed using iterative method (Successive Under Relaxation, SUR) and applying 0.1 as under-relaxation coefficient for all dependent variables. The iteration process is terminated when the following condition is satisfied:

$$\sum_{i,j} |\Phi_{i,j}^m - \Phi_{i,j}^{m-1}| \Big/ \sum_{i,j} |\Phi_{i,j}^m| \leqslant 10^{-5}, \tag{29}$$

where m denotes the iteration step and Φ stands for either θ or Ψ. Uniform grid distribution is used for whole cavity. Published experimental data are not available from the literature for the studied

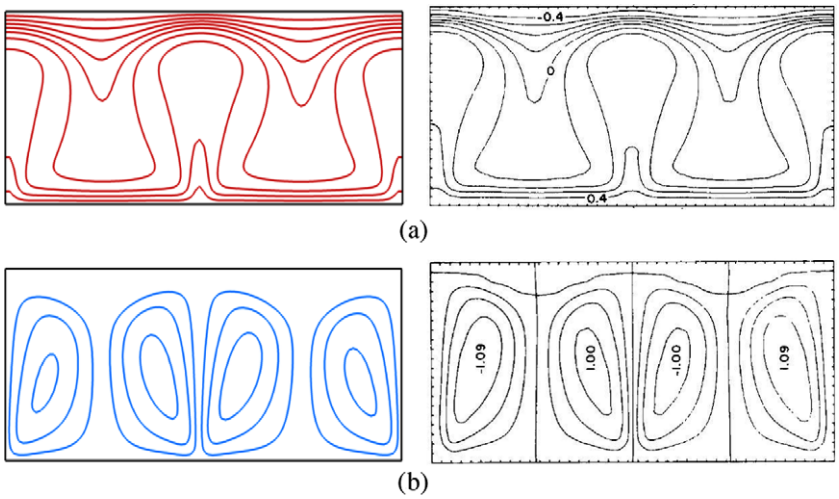

Fig. 2. Comparison of isotherms and streamlines with the literature at $Ra = 2500$: (a) isotherms for present (on the left) and Blake et al. [4] (on the right), (b) streamlines for present (on the left) and Blake et al. [4] (on the right).

enclosure configuration and boundary conditions. Thus, the validation of the obtained results against suitable experimental data could not be performed. However, a test was made to compare the results obtained by the present code with the results of earlier study of Blake et al. [4]. The obtained results are compared and shown in Fig. 2 by isotherms (on the top row) and streamlines (on the bottom row) for $Ra = 2500$ and $AR = 0.5$. It is clearly seen that the obtained results are in good agreement with the reported ones.

4. Results and discussion

The study presents results of heat and fluid flow of natural convection in a rectangular porous enclosure filled with cold water. The effects of the Rayleigh number, thickness of the bottom wall and thermal conductivity ratio on heat transfer in the enclosure are investigated for $AR = 0.5$. Results are present by streamlines, isotherms, heatline distributions and the changes of local and mean Nusselt numbers. Fig. 3 shows streamlines (left), isotherms (middle) and heatlines (right) for different values of the Rayleigh number as $Ra = 1000$, 2000 and 3000 when $\kappa = 1.0$ and $h = 0.1$. Multiple circulation cells are formed for all cases. The positive sign of Ψ denotes anti-clockwise circulation, and the clockwise circulation is represented by the negative sign of Ψ. The shape of streamlines, isotherms and heatlines are symmetry respect to the middle line of cavity ($X = L/2$). In the three cavities, two regions are seen as bottom region with circulation cells and top region with almost

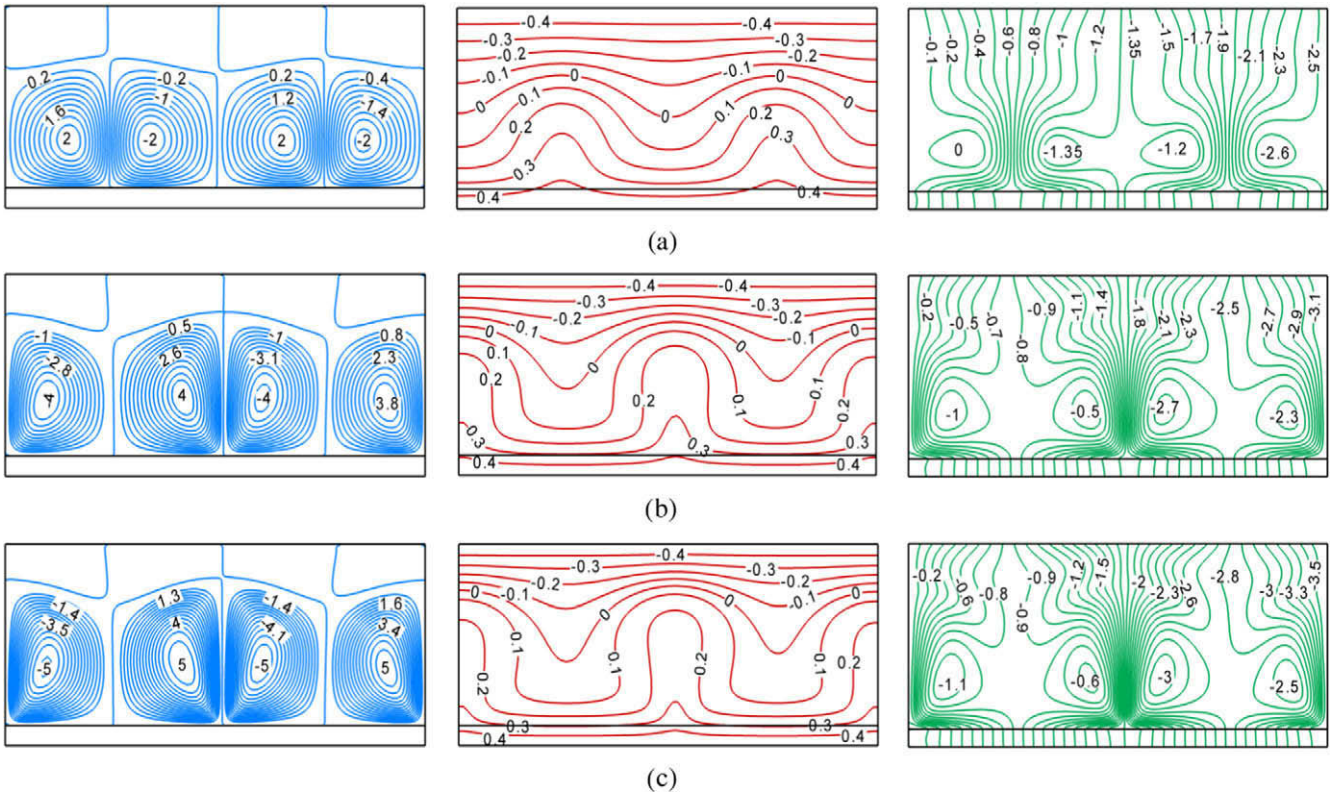

Fig. 3. Streamlines (left), isotherms (middle) and heatlines (right) for different Rayleigh numbers for $\kappa = 0.1$ and $h = 0.1$: (a) $Ra = 1000$, (b) $Ra = 2000$, and (c) $Ra = 3000$.

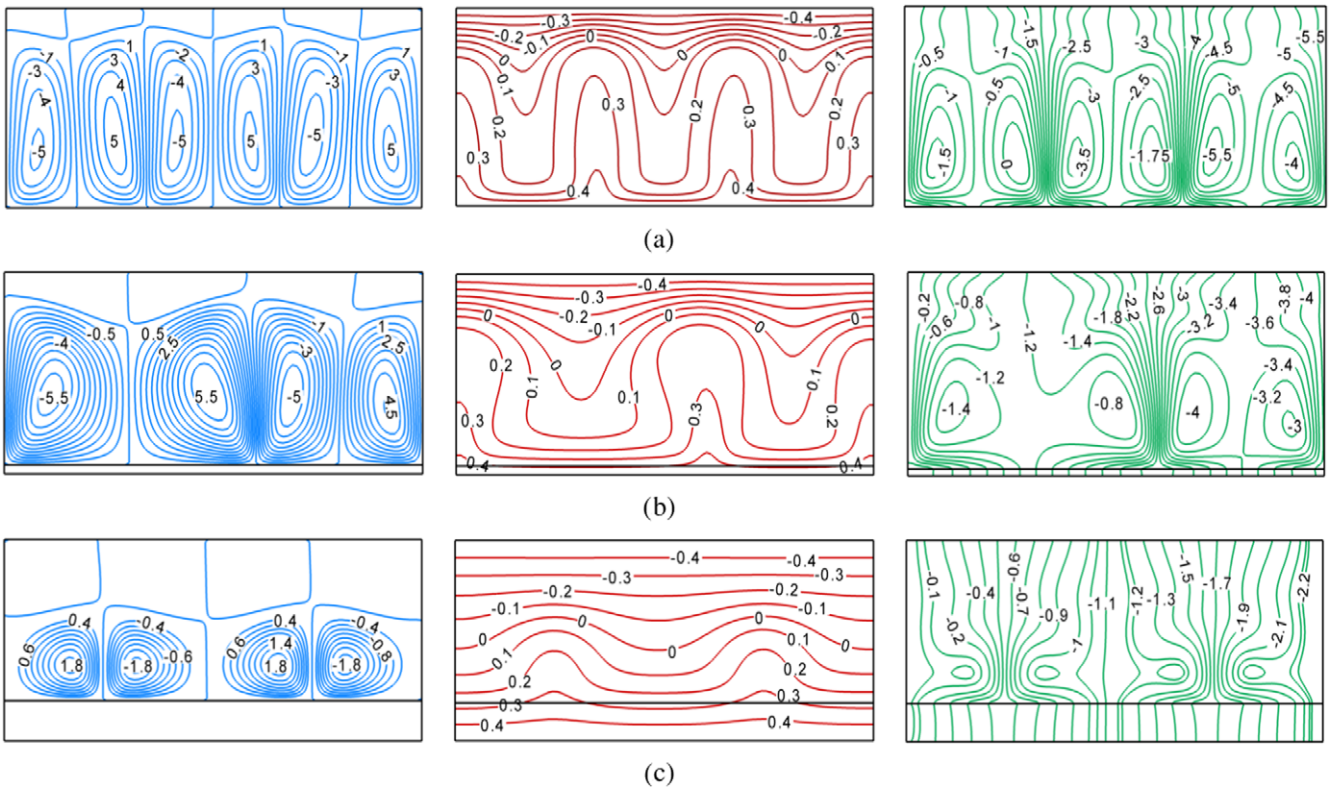

Fig. 4. Streamlines (left), isotherms (middle) and heatlines (right) for different height of thick wall $Ra = 2000$ and $\kappa = 1.0$: (a) $h = 0$, (b) $h = 0.05$, and (c) $h = 0.2$.

stagnant fluid. In the bottom region, the effect of convection heat transfer is significant and the effect of fluid flow can be seen from the isotherm patterns since they are not parallel to the floor and the flow cells distort the line shape of isotherms. However, on the top region of the cavity, the fluid is in the stagnant state and conduction heat transfer is dominant. That is why the isotherms are parallel to the ceiling and heatlines are almost perpendicular to the isotherms. The increase of Rayleigh number increases the strength of convection and isotherms are more distorted. The path of heat transfer from the bottom to the ceiling wall in solid and fluid regions can be clearly seen from the heatline patterns. In the solid wall, heatlines are parallel to the each others and parallel to the vertical walls signifying one-dimensional conduction heat transfer. In the heatline patterns of three cavities in Fig. 3, cells in which heat is only rotated is seen. These regions can be called as passive region since they do not play an important role on heat transfer from bottom to the top wall. The area of passive regions is expanded by increasing of convection strength.

Fig. 4 is displayed to investigate the floor thickness on the mechanism of heat and fluid flow. This figure shows streamlines (left), isotherms (middle) and heatlines (right) for different thick wall as $h = 0$, 0.05 and 0.2 when $Ra = 2000$ and $\kappa = 1.0$. As seen from Fig. 3, the solution is very sensitive to the parameter of thickness of bottom wall (h) and this parameter plays an important role on heat

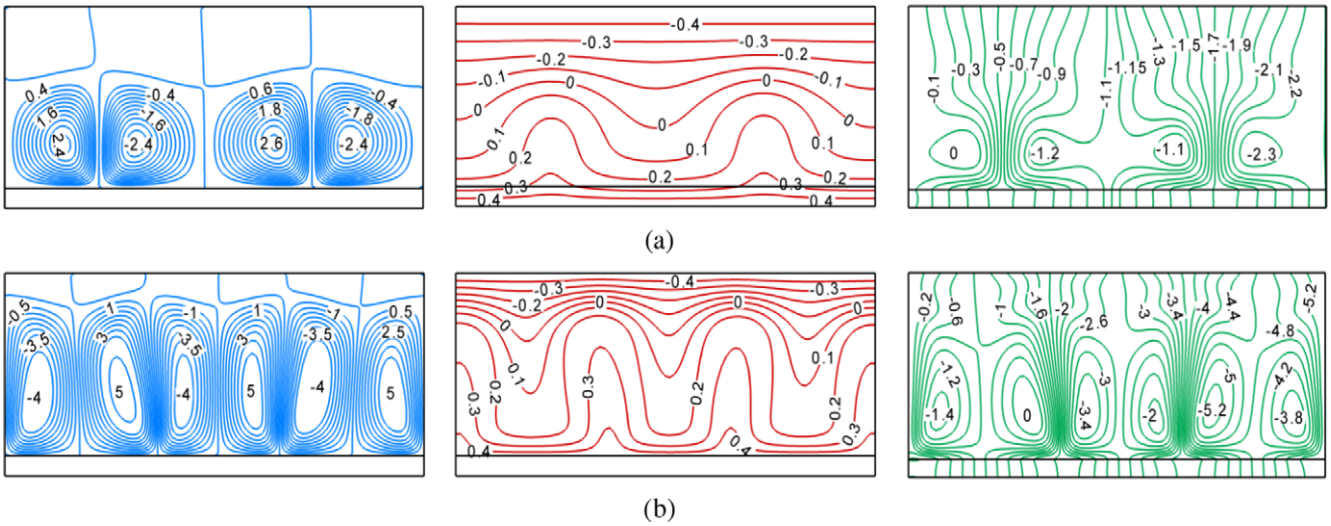

Fig. 5. Streamlines (left), isotherms (middle) and heatlines (right) for different thermal conductivity ratio $Ra = 2000$ and $h = 0.1$: (a) $k = 0.5$, (b) $\kappa = 10$.

transfer from the bottom to the top of cavity. The increase of the bottom wall thickness reduces heat transfer though the cavity and consequently decreases number of the flow cells. Similar to Fig. 3, two regions as bottom region with circulation cells and top region with stagnant fluid are seen in the cavities of Fig. 4. The increase of wall thickness reduces the strength of flow and increases the effect of conduction heat transfer. That is why the area occupied with stagnant fluid is expanded by increasing thickness of the bottom wall. For $h = 0.2$, the isotherms almost in the half region of the cavity are parallel to the top wall and heatlines are almost perpendicular to the isotherms signifying dominant conduction heat transfer in half of cavity. Again, almost one-dimensional heat transfer occurs in the solid bottom wall even in the solid wall of cavity with $h = 0.2$. The passive regions in which heat is only rotates are seen in all cavities of Fig. 4. However, the areas occupy by the passive regions decreases with increase of wall thickness.

Fig. 5 illustrates contours to see the effects of thermal conductivity on distribution of heat and fluid flow inside the cavity. As seen from the figure, thermal conductivity ratio affects the number of circulation cells due to high conductivity of the solid wall. Thus, maximum density line moves to the ceiling with increasing of thermal conductivity. However, flow strength increases due to thermal conductivity of the bottom wall. As seen from the heatlines, the area of passive regions is expanded with increasing of κ.

Fig. 6 shows the variation of local Nusselt number for solid and fluid at of $Y = 0$ and $Y = h$, respectively, for different values of Rayleigh number, thermal conductivity ratio and wall thicknesses. Fig. 6(a) shows Nu_{xs} and Nu_{xf} for the cavity with $\kappa = 1.0$ and $h = 0.1$ and for three values of Rayleigh number as 1000, 2000 and 3000. As is seen, the local solid Nusselt number is almost identical with the fluid local Nusselt number since $\kappa = 1.0$ and almost one-dimensional heat transfer exists. The local Nusselt number for solid and fluid regions are not uniform and their values are changed by location. The loca-

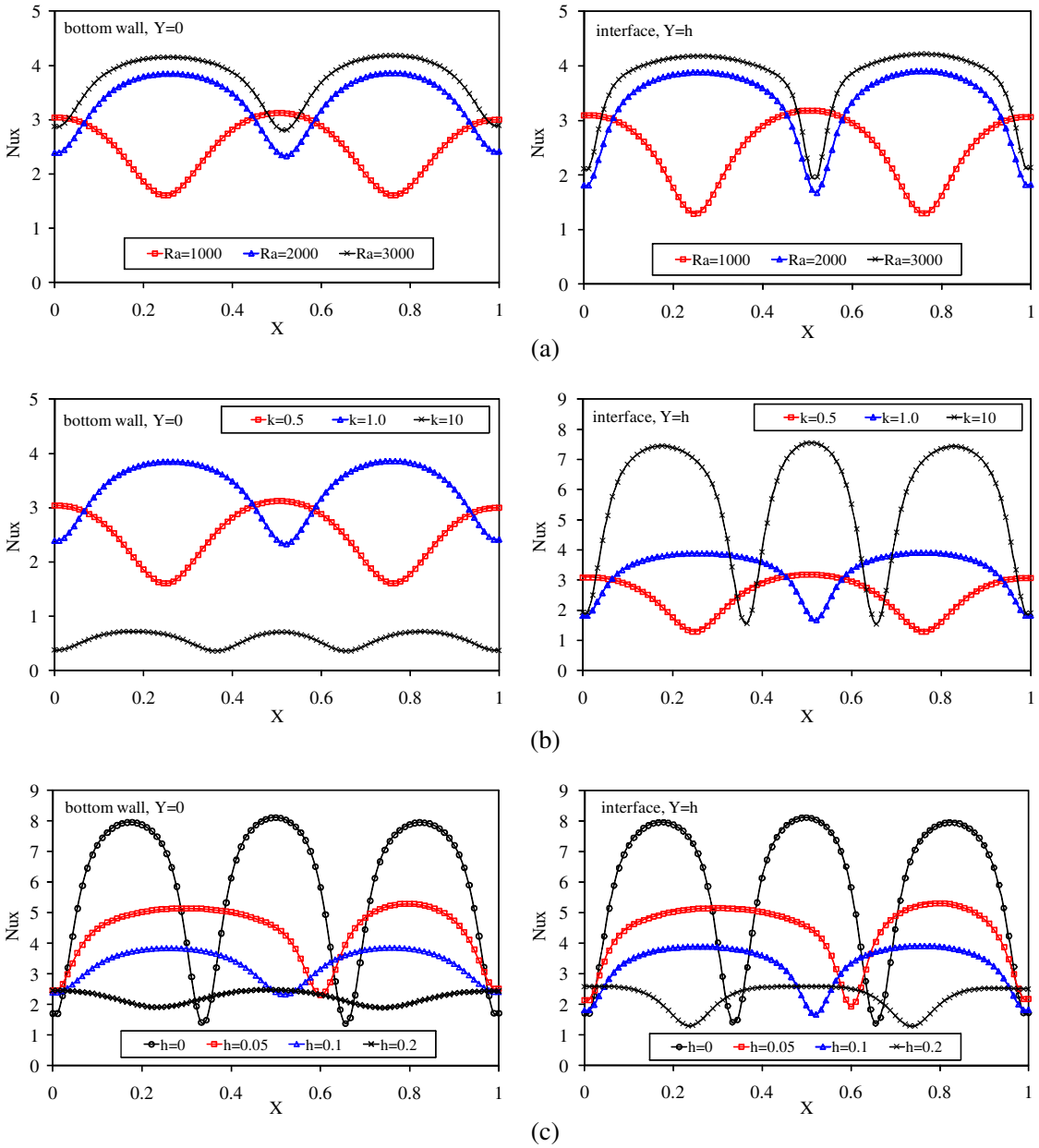

Fig. 6. Variation of local Nusselt number along the bottom wall and solid fluid interface. (a) Effects of Rayleigh number when $\kappa = 1.0$ and $h = 0.1$. (b) Effect of thermal conductivity ratio when $Ra = 2000$ and $h = 0.1$. (c) Effects of height of solid wall when $Ra = 2000$ and $\kappa = 1.0$.

tions for the minimum and maximum local Nusselt numbers for $Ra = 1000$ are different than locations of those seen for $Ra = 2000$ and 3000. The increase of the Rayleigh number increases Nusselt number and consequently heat transfer through the cavity increases. The variations of solid and fluid local Nusselt numbers for cavity with $Ra = 2000$ and $h = 0.1$ for different conductivity ratio are given in Fig. 6(b). The locations for the minimum and maximum solid and fluid local Nusselt numbers are identical signifying almost one-dimensional heat transfer in the bottom wall. Due to different values of conductivity ratio, the values of Nu_{xs} and Nu_{xf} are very different for $\kappa = 0.5$ and 10 compared to $\kappa = 1.0$. As is seen, the increase of thermal conductivity ratio increases fluid Nusselt number means that heat transfer through the cavity increases. The increase of thermal conductivity ratio reduces solid local Nusselt number and approaches to a constant value as 0.1 due to increase of one-dimensional heat transfer. Fig. 6(c) shows the variation of solid and fluid Nusselt number for different values of wall thickness. The increase of bottom wall thickness reduces solid and fluid Nusselt numbers. Again, the variations of the solid and fluid Nusselt numbers are similar to each other since $\kappa = 1.0$.

The variations of fluid mean Nusselt number with Rayleigh number for different thickness of bottom wall are shown in Fig. 7. For Rayleigh number around 500, conduction heat transfer is the dominant mode of heat transfer in the cavity for different values of bottom wall thickness. That is why the gradient of the dimensionless temperature along the vertical direction of the cavity is identical for the different wall thickness. The increase of the Rayleigh number enhances convection effect and hence mean Nusselt numbers for different wall thickness become different. As is seen in Fig. 7, the increase of the bottom wall thickness reduces fluid mean Nusselt number. By adding dimensionless wall thickness as $h = 0.2$ and $\kappa = 1.0$ to the bottom of a cavity with $Ra = 5000$, the mean Nusselt number of the cavity is reduced.

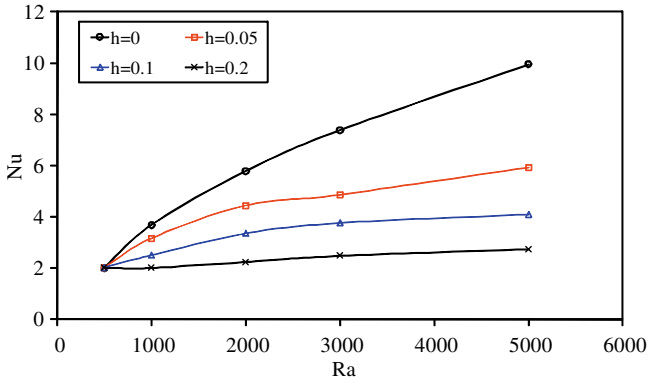

Fig. 7. Variation of mean Nusselt number for different Rayleigh number at different height of thick wall when $\kappa = 1.0$.

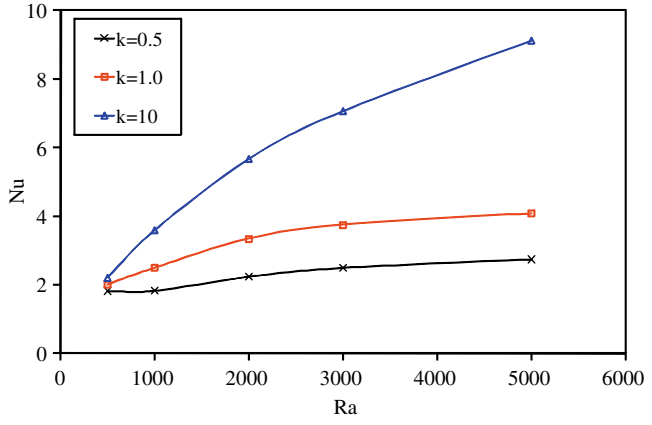

Fig. 8. Variation of mean Nusselt number for different Rayleigh number at different thermal conductivity ratio when $h = 0.1$.

Fig. 8 shows the change of the fluid mean Nusselt number with Rayleigh for different values of thermal conductivity ratio. Similar to Fig. 6, for low values of Rayleigh number, the values of Nu_f are almost same due to dominant conduction mode of heat transfer. The increase of the conductivity ratio increases the value of Nu_f and consequently heat transfer through the cavity increases. For an enclosure with bottom wall thickness as $h = 0.1$ and $Ra = 5000$, the increase of thermal conductivity ratio from 0.5 to 10 increases 3.33 times the fluid Nusselt number.

5. Conclusions

A numerical study was conducted on conduction-natural convection heat transfer and fluid flow for cold water in an enclosure with finite bottom wall and filled with porous medium. The study was performed for different values of Rayleigh number, thermal conductivity ratio and thickness of bottom wall. Heatline visualization technique was used to present the path of heat flow from the bottom to the top wall. The obtained results show that the bottom wall plays a heat barrier role on the heat transfer through the cavity. The increase of conductivity ratio ($\kappa = k_s/k_f$) enhances heat transfer rate, however, the increase of the bottom wall thickness reduces natural convection from the bottom to the top wall. Similar to the other natural convection heat transfer problems, the increase of the Rayleigh number enhances the strength of the heat and flow and consequently Nusselt number increases. Generally two regions are observed in the cavity. In the bottom region of the cavity circulation cells form while fluid is in stagnant state in the top region. Heatline visualization technique was successfully applied to the problem to demonstrate the path of heat transfer in both solid and fluid regions.

Acknowledgements

The authors express their very sincere thanks to the reviewers for their valuable comments and suggestions.

References

[1] D.A. Nield, A. Bejan, Convection in Porous Media, second ed., Springer, New York, 1999.
[2] D.B. Ingham, I. Pop (Eds.), Transport Phenomena in Porous Media, vol. II, Pergamon Press, Oxford, 2002.
[3] J. Boussinesq, Theorie Analytique de la Chaleur, vol. II, Gauthier-Villars, Paris, 1903.
[4] K.R. Blake, A. Bejan, D. Poulikakos, Natural convection near 4 °C in a water saturated porous layer heated from below, Int. J. Heat Mass Transfer 27 (1984) 2355–2364.
[5] N.H. Saeid, I. Pop, Maximum density effects on natural convection from a discrete heater in a cavity filled with a porous medium, Acta Mech. 171 (2004) 203–212.
[6] S. Sivasankaran, C.J. Ho, Effect of temperature dependent properties on natural convection of water near its density maximum in enclosures, Numer. Heat Transfer, Part A 53 (2008) 507–523.
[7] R.A. Osorio, R. Avila, J. Cervantes, On the natural convection of water near its density inversion in an inclined square cavity, Int. J. Heat Mass Transfer 47 (2004) 4491–4495.
[8] H. Inaba, T. Fukuda, Natural convection in a square cavity in regions of density inversion of water, J. Fluid Mech. 142 (1984) 363–381.
[9] D.S. Lin, M.W. Nansteel, Natural convection heat transfer in a square enclosure containing water near its density maximum, Int. J. Heat Mass Transfer 30 (1987) 2319–2329.
[10] C.J. Ho, F.J. Tu, Visualization and prediction of natural convection of water near its density maximum in a tall rectangular enclosure at high Rayleigh numbers, Trans. ASME J. Heat Transfer 123 (2001) 84–95.
[11] N.H. Saeid, Conjugate natural convection in a porous enclosure: effect of conduction in one of the vertical walls, Int. J. Therm. Sci. 46 (2007) 531–539.

[12] A.C. Baytas, A. Liaqat, T. Groşan, I. Pop, Conjugate natural convection in a square cavity, Heat Mass Transfer 37 (2001) 467–473.
[13] A. Al-Amiri, K. Khanafer, I. Pop, Steady-state conjugate natural convection in a fluid-saturated porous cavity, Int. J. Heat Mass Transfer 51 (2008) 4260–4275.
[14] W.J. Chang, H.C. Lin, Wall heat conduction effect on natural convection in an enclosure filled with a non-Darcian porous medium, Numer. Heat Transfer, Part A 25 (1994) 671–684.
[15] S. Kimura, A. Bejan, The heatline visualization of convective heat transfer, Trans. ASME J. Heat Transfer 105 (1983) 916–919.
[16] V.A.F. Costa, Bejan's heatlines and masslines for convection visualization and analysis, Appl. Mech. Rev. 59 (2006) 126–145.
[17] E. Hakyemez, M. Mobedi, H. Oztop, Effects of wall-located heat barrier on conjugate conduction/natural-convection heat transfer and fluid flow in enclosures, Numer. Heat Transfer, Part A 54 (2008) 197–220.
[18] S.L. Goren, On free convection in water at 4 °C, Chem. Eng. Sci. 21 (1966) 515–518.
[19] D.R. Moore, N.O. Weiss, Nonlinear penetrative convection, J. Fluid Mech. 61 (1973) 553–581.
[20] H.F. Oztop, Y. Varol, I. Pop, Investigation of natural convection in triangular enclosure filled with porous medium saturated with water near 4 °C, Energy Convers. Manage. 50 (2009) 1473–1480.
[21] Y. Varol, H.F. Oztop, I. Pop, Maximum density effects on buoyancy-driven convection in a porous trapezoidal cavity, Int. Commun. Heat Mass Transfer (2009), doi:10.1016/j.icheatmasstransfer.2009.11.003.
[22] Y. Varol, H.F. Oztop, M. Mobedi, I. Pop, Visualization of natural convection heat transport using heatline method in porous non-isothermally heated triangular cavity, Int. J. Heat Mass Transfer 51 (2008) 5040–5051.